



OPEN

Phytosulfokine α (PSK α) delays senescence and reinforces SUMO1/SUMO E3 ligase SIZ1 signaling pathway in cut rose flowers (*Rosa hybrida* cv. Angelina)

Morteza Soleimani Aghdam^{1✉}, Amin Ebrahimi² & Morteza Sheikh-Assadi³

Roses are widely used as cut flowers worldwide. Petal senescence confines the decorative quality of cut rose flowers, an impressively considerable economic loss. Herein, we investigated the SUMO1/SUMO E3 ligase SIZ1 signaling pathway during bud opening, and petal senescence of cut rose flowers. Our results exhibited that the higher expression of *SUMO1* and *SUMO E3 ligase SIZ1* during bud opening was accompanied by lower endogenous H₂O₂ accumulation arising from higher expression and activities of *SOD*, *CAT*, *APX*, and *GR*, promoting proline accumulation by increasing *P5CS* expression and activity and enhancing GABA accumulation by increasing *GAD* expression and activity. In harvested flowers, lower expressions of *SUMO1* and *SUMO E3 ligase SIZ1* during petal senescence were associated with higher endogenous H₂O₂ accumulation due to lower expression and activities of *SOD*, *CAT*, *APX*, and *GR*. Therefore, promoting the activity of the GABA shunt pathway as realized by higher expression and activities of *GABA-T* and *SSADH* accompanied by increasing *OAT* expression and activity for sufficiently supply proline in rose flowers during petal senescence might serve as an endogenous antisenesescence mechanism for slowing down petals senescence by avoiding endogenous H₂O₂ accumulation. Following phytosulfokine α (PSK α) application, postponing petal senescence in cut rose flowers could be ascribed to higher expression of *SUMO1* and *SUMO E3 ligase SIZ1* accompanied by higher expression and activities of *SOD*, *CAT*, *APX*, and *GR*, higher activity of GABA shunt pathway as realized by higher expression and activities of *GAD*, *GABA-T*, and *SSADH*, higher expression and activities of *P5CS* and *OAT* for supplying proline and higher expression of *HSP70* and *HSP90*. Therefore, our results highlight the potential of the PSK α as a promising antisenesescence signaling peptide in the floriculture industry for postponing senescence and extending the vase life of cut rose flowers.

Rose flowers (*Rosa hybrida*) are extensively used as cut flowers worldwide. Petal senescence confines the decorative quality of cut rose flowers, an impressively considerable economic loss. Therefore, revealing mechanisms regulating rose flowers' bud opening and petal senescence would be advantageous for introducing an innovative approach for extending the vase life of cut rose flowers¹.

In plants, SUMO E3 ligase SIZ1 is accountable for the reversible attachment of small ubiquitin-like modifier (SUMO) peptides to target proteins. As a reversible post-translational modification (PTM), SUMOylation regulates plant development and stress responses by holding protein stability, enzymatic activity, subcellular location, and protein–protein interactions². The following are required for SUMOylation: (1) maturation of SUMO peptide by SUMO endopeptidase; (2) SUMO activation by hydrolyzing ATP via E1 SUMO activation enzymes³ (3) SUMO conjugation by E2 SUMO conjugation enzymes; and (4) ligation by E3 SUMO ligase SIZ1 for the attachment of SUMO peptide to a lysine residue of target proteins. In addition, the SUMO isopeptidase enzyme is accountable for deSUMOylation by releasing and recycling SUMO from proteins. Moreover, following

¹Department of Horticultural Science, Imam Khomeini International University, 34148-96818 Qazvin, Iran. ²Department of Agriculture and Plant Breeding, Faculty of Agriculture, Shahrood University of Technology, Semnan, Iran. ³Department of Horticultural Science, University College of Agriculture and Natural Resources, University of Tehran, Karaj, Iran. ✉email: soleimaniaghdam@eng.ikiu.ac.ir

the activity of SUMO E4 ligase, polySUMOylation is responsible for the ubiquitination of proteins, which are degraded by ubiquitin E4 ligases. E3 SUMO ligase SIZ1 promotes the activity of E3 ubiquitin ligase COP1 by SUMOylation, whereas E3 ubiquitin ligase COP1 suppresses it by ubiquitination^{2,3}. During senescence and stresses, inducer of CBF expression 1/C-repeat binding factors (ICE1/CBFs) signaling pathway^{4,5}, heat shock transcription factors/heat shock proteins (HSFs/HSPs) signaling pathway^{6,7}, sugar sensing, and signaling by the target of rapamycin/sucrose non-fermenting 1 (SNF1)-related kinase 1 (TOR/SnRK1) signaling pathway⁸, and nitrate reductase/R2R3-MYB transcription factors (NR/MYBs) signaling pathway^{9–14} by SUMO E3 ligase SIZ1 might be accountable for regulating plant growth and development and stress responses.

As a plant peptide hormone, phytosulfokine α (PSK α ; Tyr(SO₃H)-Ile-Tyr(SO₃H)-Thr-Gln) has been employed to palliate chilling injury and fungal decay, delay senescence, and preserve sensory and nutritional quality in fruits and vegetables during postharvest life. Following the application of PSK α , the activation of a cytosolic cGMP signaling pathway^{15,16} was accompanied by the promotion of the extracellular ATP signaling pathway¹⁷, increasing the activities of intracellular SnRK1 and SUMO E3 ligase SIZ1 signaling pathways^{18,19}, promoting that of arginase/nitric oxide synthase (ARG/NOS) pathway²⁰, and suppressing that of poly(ADP-Ribose) polymerase 1 (PARP1) signaling pathway²¹. Following PSK α application, there is sufficient NADPH and ATP (intracellular reducing power and energy currency) provision^{18,21}, which increases the activities of reactive oxygen species (ROS) avoiding and scavenging systems^{17,18}. This activates the accumulation of endogenous melatonin¹⁵, hydrogen sulfide²², cytokinin¹⁹, γ -aminobutyric acid (GABA), proline, nitric oxide, and polyamines²⁰, enhancing the activities of intracellular molecular chaperone and protein repairing systems^{17,19}, suppressing ethylene biosynthesis and chlorophyll degradation²², improving ABTS, FRAP, and DPPH scavenging capacity due to the accumulation of phenols, flavonoids, anthocyanins, and ascorbic acid^{15,16}. These help preserve membrane integrity as realized by lower electrolyte leakage and malondialdehyde (MDA) accumulation, which might be accountable for palliating chilling injury and fungal decay, postponing senescence, and preserving sensory and nutritional quality in fruits and vegetables during postharvest life²³.

This study elucidates the endogenous SUMO1/SUMO E3 ligase SIZ1 signaling pathway during bud opening and petal senescence of rose flowers. Furthermore, the potential of PSK α treatment for delaying senescence and prolonging vase life of cut rose flowers was evaluated by studying (1) *SUMO1* and *SUMO E3 ligase SIZ1* genes expression, (2) endogenous accumulation of H₂O₂ by gene expression and activities of superoxide dismutase (SOD), catalase (CAT), ascorbate peroxidase (APX), and glutathione reductase (GR); (3) endogenous accumulation of proline by gene expression and activities of pyrroline-5-carboxylate synthase (P5CS) and ornithine aminotransferase (OAT); (4) activity of endogenous GABA shunt pathway by gene expression and activities of glutamate decarboxylase (GAD), GABA transaminase (GABA-T), and succinate semialdehyde dehydrogenase (SSADH) as well as the expression of heat shock proteins 70/90 (HSP70/90).

Materials and methods

SUMO E3 ligase SIZ1 signaling pathway during bud opening and petal senescence of rose flowers. For illustrating the SUMO E3 ligase SIZ1 signaling pathway during bud opening and petal senescence, commercial cut rose flowers (*Rosa hybrida* cv. Angelina) were obtained from a legalized local commercial greenhouse in Qazvin Province, Iran. All protocols were complied with relevant institutional, national, and international guidelines and legislation. For developmental stage 1, closed buds; stage 2, closed and heavily pigmented bud; and stage 3, flowers with their outer petal whorl just unfurled as commercial harvest stage, outermost-to-innermost petals from 10 flowers in three replications (30 flowers, 10 flowers per replication) were harvested according to Aghdam et al.¹. After harvesting at the commercial stage (stage 3), flowers were re-cut underwater to a stem length of 40 cm to avoid air embolism, with six leaves. Flowers were placed randomly in 1000 mL distilled water for 12 days in three replications (30 flowers, 10 flowers per replication). During vase life at 20 ± 1 °C and 60 ± 5% relative humidity, petals were harvested from the flowers at stage 4, sepals completely opened, petal starting to unfold (flowers 4 days after harvest); stage 5, petals completely unfolded (flowers 8 days after harvest); and stage 6, flowers completely senesced with petal bluing (flowers 12 days after harvest). The vase solution was replaced with fresh distilled water every day. For developmental stages 4–6, outermost-to-innermost petals from 10 flowers were harvested, according to Aghdam et al.¹.

Rose flowers and PSK α treatment. Regarding longest vase life, 16 days for PSK α at 150 nM in comparison with 12 days for PSK α at 0 nM as reported by Aghdam et al.¹, 180 flowers (*Rosa hybrida* cv. Angelina) harvested at commercial-stage (stage 3), was re-cut underwater to a stem-length of 40 cm to avoid air embolism, with six leaves. Flowers were placed randomly in 1000 mL distilled water or PSK α at 150 nM for 24 h as pulse treatment. PSK α (soluble in sterile water; 1 mg/mL) was provided by Pepmic Co., Ltd, Suzhou (China). After pulse treatment for 24 h, the vase solution was replaced with fresh distilled water for 4, 8, and 12 days, in three replications, respectively (90 flowers, 30 flowers per replication, 10 flowers per sampling time). During vase life at 4, 8, and 12 days after harvest, outermost-to-innermost petals from 10 flowers were harvested, according to Aghdam et al.¹. During developmental stages and vase life, petals harvested from flowers were immediately frozen in liquid nitrogen, powdered, and stored at –80 °C for biochemical and gene expression analysis.

Activities of SOD, CAT, APX, and GR and endogenous H₂O₂ accumulation. To analyze the SOD, CAT, APX, and GR activities, five grams of the frozen powder was homogenized with 25 mL of phosphate buffer (50 mM; pH 7.8) containing 0.2 mM EDTA and 2% PVP. SOD, CAT, APX, and GR enzymes activity were determined according to Giannopolitis and Ries²⁴, Beers and Sizer²⁵, Nakano and Asada²⁶, and Sofu et al.²⁷, respectively. For CAT activity, 100 μ L of the enzyme extract was added to 2.9 mL of reaction mixture containing 15 mM H₂O₂ and 50 mM phosphate buffer (pH 7). The degradation of H₂O₂ was measured by the decrease of

absorbance at 240 nm during 1 min. One unit of CAT activity was defined as a decrease in absorbance at 240 nm of 0.01 per min. For APX activity, 100 μL of the enzyme extract was added to 2.9 mL of reaction mixture containing 50 mM phosphate buffer (pH 7), 0.5 mM ascorbic acid and 1 mM H_2O_2 . The decrease of absorbance at 290 nm during 1 min was measured. One unit of APX activity was defined as the enzyme that oxidizes 1 μmol of ascorbate per minute. For SOD activity, 100 μL of enzyme extract was added to 2.9 mL of reaction mixture containing 50 mM phosphate buffer (pH 7), 5 mM methionine, 100 μM EDTA, 65 μM NBT, and 40 μL of 0.15 mM riboflavin. The tubes were then placed in a fluorescent light incubator (40 W, 10 min), and the formation of blue formazan was monitored by recording the absorbance at 560 nm. One unit of SOD activity is defined as the enzyme that causes a 50% inhibition of NBT reduction under assay conditions. For GR activity based on the decrease in absorbance at 340 nm due to NADPH oxidation, 200 μL of enzyme extract was added to a reaction mixture containing 1.5 mL of 0.1 M phosphate buffer (pH 7), 150 μL of 20 mM GSSG, 1 mL of distilled water and 150 μL of 2 mM NADPH (dissolved in Tris-HCl buffer, pH 7), in a final volume of 3.0 mL. One unit of GR activity was defined as the enzyme that oxidizes 1 nmol of NADPH per min at 25 °C. Their activities were expressed as U kg^{-1} protein. The endogenous H_2O_2 accumulation was assayed following titanium (IV) procedure according to Patterson et al.²⁸. One gram of the frozen powder was homogenized with 5 mL of acetone at 0 °C. After centrifugation for 15 min at 6000 \times g at 4 °C, the supernatant was collected. The supernatant (1 mL) was mixed with 0.1 mL of 5% titanium sulfate and 0.2 mL ammonia and then centrifuged for 10 min at 6000 \times g at 4 °C. The pellets were dissolved in 3 mL of 10% (v/v) H_2SO_4 and centrifuged for 10 min at 5000 \times g at 4 °C. The absorbance of the supernatant was measured at 410 nm. The endogenous H_2O_2 accumulation was expressed as $\mu\text{mol kg}^{-1}$ on a fresh weight basis.

Activities of P5CS and OAT and endogenous proline accumulation. According to Zhang et al. (2013), the endogenous proline accumulation was measured following the acid ninhydrin method. One gram of the frozen powder was homogenized in 5 mL of 3% (v/v) sulfosalicylic acid and centrifuged at 12,000 \times g for 10 min. Two mL of glacial acetic acid and 3 mL of ninhydrin reagent were mixed with supernatant (2 mL) and boiled for 10 min. Then 4 mL of toluene was added into the reaction mixture after the solution was cooled. The absorbance of the organic phase was recorded at 520 nm. The endogenous proline accumulation was expressed as mmol kg^{-1} on a fresh weight basis. For OAT activity, according to Shan et al.²⁹, the reaction mixture contained 35 mM l-ornithine, 0.05 mM PLP, 25 mM α -ketoglutarate, and the enzyme extract. The mixture was incubated at 37 °C for 20 min before adding 3M HClO_4 . Then, 2% ninhydrin was added into the mixture and boiled for 20 min. After cooling, the mixture was centrifuged at 15,000 \times g for 10 min. The residue was dissolved in 2 mL toluene and quantified by measuring the absorbance at 510 nm. For P5CS activity according to Shan et al.²⁹, the reaction mixture contained 100 mM Tris-HCl (pH 7.2), 25 mM MgCl_2 , 75 mM sodium glutamate, 5 mM ATP, 0.4 mM NADPH and 200 μL enzyme extract. One unit of P5CS and OAT enzymes activity was defined as an enzyme that caused a decrease by 0.001 in an absorbance per minute at 340 nm. P5CS and OAT activity were expressed as U kg^{-1} protein.

Activities of GAD, GABA-T, and SSADH and endogenous GABA accumulation. The enzymatic assay with GABase was employed to quantify GABA accumulation described by Deewatthanawong et al.³⁰. For endogenous GABA accumulation assessment, one gram of the frozen powder was homogenized in 5 mL of methanol for 10 min at room temperature. After vacuum dried, dissolved in 1 mL 70 mM lanthanum chloride followed by 15 min of shaking, and centrifugation at 13,000 \times g for 15 min. Then, 800 μL supernatant was mixed with 160 μL 1M KOH. After being shaken for 5 min, and centrifugation at 13,000 \times g for 10 min, the supernatant was used for GABA determination. The GABase assay mixture contained 75 mM potassium pyrophosphate (pH 8.6), 3.3 mM β -mercaptoethanol, 10 mM 2-oxoglutarate, 1.25 mM NADP^+ , and 0.016-unit GABase. The absorbance at 340 nm was read before, and 10 min after adding α -ketoglutarate using the 96-well plate reader, and GABA was determined by comparison with a standard curve of GABA. GABA accumulation was expressed as mmol kg^{-1} fresh weight.

GAD, GABA-T, and SSADH activity were determined according to Bartyzel et al.³¹, Ansari et al.³², and Thornburn et al.³³. For GAD, GABA-T and SSADH extraction, two grams of the frozen powder was homogenized in 12 mL of 0.1 M Tris-HCl buffer (pH 9.1) containing 5 mM EDTA, 1 mM phenylmethylsulfonyl fluoride (PMSF), 1 mM dithiothreitol (DTT), 10% (v/v) glycerol, 0.5 mM pyridoxal phosphate (PLP) and 0.1% polyvinylpyrrolidone (w/v) (PVPP). The homogenate was centrifuged at 10,000 \times g for 15 min at 4 °C and the supernatant was filtered and concentrated with Amicon Ultra centrifugal filters 10,000 MWCO (Millipore®). Then, it was re-suspended in 1.5 mL of 0.2 M sodium phosphate buffer (pH 5.8) containing 0.04 mM PLP for GAD activity, or in 1.5 mL of 50 mM Tris-HCl buffer (pH 8.2) containing 0.75 mM EDTA, 1.5 mM DTT, 10% (v/v) glycerol, 0.2 mM PLP for GABA-T activity or in 1.5 mL of 0.1M sodium phosphate buffer (pH 9) containing 1 mM DTT and 1 mM EDTA for SSADH activity. Activities of GAD, GABA-T, and SSADH enzymes were analyzed based on the production of GABA, alanine, and succinate and expressed as $\mu\text{mol GABA}$ or alanine or succinate kg^{-1} protein min^{-1} .

Gene expression analysis by quantitative real-time PCR. Total RNA was isolated from petals using the RNeasy Plant Mini Kit (Qiagen, Hilden, Germany). Then, gel electrophoresis by 1% agarose gel and absorbance at 260 nm by NanoDrop spectrophotometer (BioTek, EPOCH, serial 121004C, USA) was used for evaluating RNA quality and quantity. After RNase-free DNaseI (Thermo Fisher Scientific) treatment, one μg RNA was applied to synthesize the first-strand cDNA HyperscriptTM Reverse Transcriptase (GeneAll Inc, South Korea). Real-time quantitative PCR was fulfilled by BioRad system (Bio-Rad, Hercules, CA, USA) using the SYBR Green PCR Master Mix 2X (Amplicon, Denmark). The primers used to amplify the gene sequences are listed in Table 1.

Gene name	Accession numbers	Functional annotations	Primer sequences (5'–3')
<i>SUMO1</i>	XM024336892	Protein SUMOylation	F: TCTTCGGGCCTTTAGAACCT R: TCAGTTCAGGGTTTGGGTTT
<i>SIZ1</i>	XM040519042	Protein SUMOylation	F: GCTGAACCTGCAGACACAAA R: CAGATACACTCGCGGTCTCA
<i>SOD</i>	KJ159890	ROS scavenging	F: ATCGTGGATAGCCAGATACCA R: CAACCACACCACATGCCAATC
<i>CAT</i>	MF667950	ROS scavenging	F: TGTGCACACCTACCGAATGA R: CATCAGCTCCTCGCATCGTC
<i>APX</i>	KY274158	ROS scavenging	F: TTGTGCTCTACTCGTGCCAG R: TGACGGTTGGGTAGCACTTC
<i>GR</i>	MF667955	ROS scavenging	F: GTCATCCGCATGGAGCACTA R: GCACAGGTCTCGAAAGTCCA
<i>P5CS</i>	XM024334137	Proline biosynthesis	F: AGCAATAAACTGGTTTCTCAA R: GCCATATCCATATTAGCAGAC
<i>OAT</i>	XM024318202	Proline biosynthesis	F: GATGAAATACAATCTGGTTTAGC R: CCGCACTTACAGGTATCA
<i>GAD</i>	XM024333661	GABA shunt pathway	F: GAGGTGAAGTTGAGGGATGATT R: CATTAAAGAGTGAACCGAGGATAG
<i>GABA-T</i>	XR005804965	GABA shunt pathway	F: AGAAGTCAGAGGGTAGCTATGT R: CCACTAGTCGAGGCTCATTTTC
<i>SSADH</i>	XM024304033	GABA shunt pathway	F: GCAAGTCCCGAGGTAAGAAA R: TGCCACCAAGTTCAAGAGATAC
<i>HSP70</i>	XM024321184	Molecular chaperones	F: GTGCTACAAGGTGAGCGTGA R: GCTCTGCTCTGGCAGAAAC
<i>HSP90</i>	XP024185377	Molecular chaperones	F: GGAAGTGTAACCCTGCCAAA R: CAAGCTCTCGAAGGAACACC
<i>Actin</i>	AF044573	Housekeeping gene	F: CCATGAGACCACATACAATTCG R: CAGCAGTAAGCCTACAAGTTCATA

Table 1. Primers used for qRT-PCR.

The threshold cycle (Ct) value was normalized to Actin Ct value as a housekeeping gene¹. The relative expression of the gene was calculated by formula $2^{-\Delta\Delta Ct}$ according to Livak and Schmittgen³⁴.

Statistical analysis. The experiment was planned using a factorial design with three biological replications and two factors: PSK α treatments (0 and 150 nM PSK α) and vase life duration (4, 8, and 12 days). Three technical replications were carried out by three extractions from each biological replication for biochemical and gene expression analyses to avoid the instrumental error. The means of three technical replications are considered as one biological replication. All analyses were performed by using SPSS software³⁵ version 21 (IBM SPSS: Chicago, IL, USA). The heat map of genes expression in rose flowers during opening and senescence was created in R using the Pheatmap package³⁶. All data were expressed as mean \pm standard error (SE) from three biological replications. Fisher's least significant differences (LSD) tests were performed to compare differences between mean values at $P < 0.05$.

Results

SUMO1/SUMO E3 ligase SIZ1 signaling pathway during flower bud opening. As shown in Fig. 1, rose flowers exhibited higher expression of *SUMO1* and *SUMO E3 ligase SIZ1* ($P < 0.01$) during bud opening. Matching with higher SUMO1/SUMO E3 ligase SIZ1 genes expression, higher expression and activities ($P < 0.01$) of *SOD*, *CAT*, *APX*, and *GR* were associated with lower endogenous H₂O₂ accumulation ($P < 0.01$) in rose flowers during bud opening (Fig. 1; Table 2). In addition, higher endogenous proline (Table 3) and GABA accumulation (Table 4) ($P < 0.01$) in rose flowers during bud opening was concomitant with higher expression and activity *P5CS* and *GAD*, respectively (Fig. 1; Tables 3 and 4) ($P < 0.01$).

SUMO1/SUMO E3 ligase SIZ1 signaling pathway during petal senescence. Harvested rose flowers exhibited lower expression of *SUMO1* and *SUMO E3 ligase SIZ1* (Fig. 1; $P < 0.01$). Matching with lower SUMO1/SUMO E3 ligase SIZ1 signaling pathway, lower expression and activities of *SOD*, *CAT*, *APX*, and *GR* ($P < 0.01$) were associated with higher endogenous H₂O₂ accumulation ($P < 0.01$) in cut rose flowers during petal senescence (Fig. 1; Table 2). Also, cut rose flowers during petal senescence exhibited lower expression and activity of *P5CS* ($P < 0.01$) concomitant with higher expression and activity of *OAT* ($P < 0.01$), thereby activating endogenous proline accumulation ($P < 0.01$) in cut rose flowers during petal senescence (Fig. 1; Table 3). In addition, lower GABA accumulation in cut rose flowers during petal senescence was associated with higher expression and activities of *GABA-T* and *SSADH* ($P < 0.01$) (Fig. 1; Table 4).

PSK α treatment and petal senescence in cut rose flowers. As shown in Fig. 2, reinforcing the expression of *SUMO1* and *SUMO E3 ligase SIZ1* ($P < 0.01$) by 150 nM PSK α treatment might postpone senes-

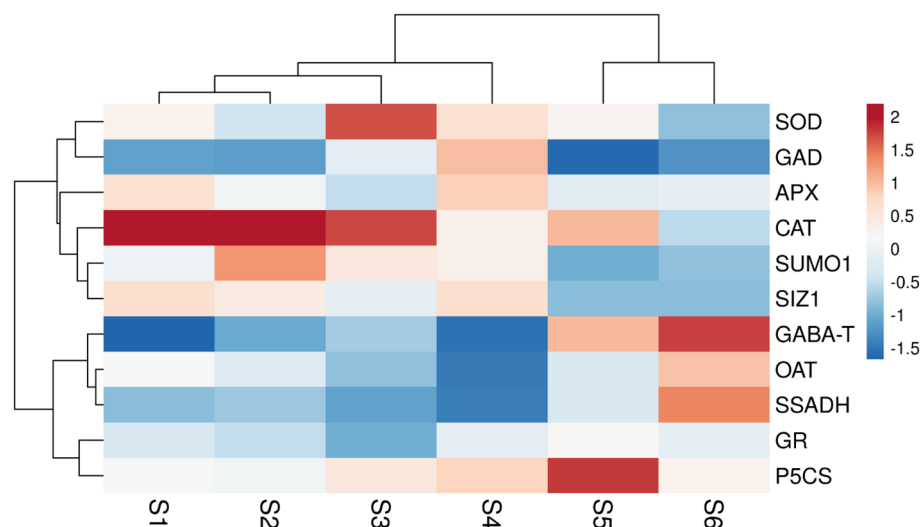


Figure 1. Heat map was created in R using the pheatmap package for representing *SUMO1/SIZ1* accompanying ROS scavenging, proline biosynthesis and GABA shunt pathway genes expression in rose flowers during opening and senescence. Stage 1, closed buds; stage 2, closed and heavily pigmented bud; and stage 3, flower with their outer petal whorl just unfurled as commercial harvest stage, stage 4, sepals completely opened, petal starting to unfold (4 days after harvest); stage 5, petals completely unfolded (8 days after harvest); and stage 6, flower completely senesced with petal bluing (12 days after harvest).

Flower development stages	SOD activity (U kg ⁻¹)	CAT activity (U kg ⁻¹)	APX activity (U kg ⁻¹)	GR activity (U kg ⁻¹)	H ₂ O ₂ accumulation (μmol kg ⁻¹ FW)
Stage 1	35.29 ± 2.37 d	88.18 ± 5.14 b	18.97 ± 1.30 c	12.36 ± 1.01 c	15.60 ± 0.84 c
Stage 2	43.36 ± 3.35 d	115.50 ± 7.79 a	22.47 ± 1.62 c	17.87 ± 1.85 c	19.71 ± 2.09 c
Stage 3	69.42 ± 5.37 c	128.74 ± 6.03 a	48.73 ± 4.23 b	38.34 ± 3.45 a	22.80 ± 1.93 c
Stage 4	128.74 ± 5.73 a	113.33 ± 7.37 a	69.83 ± 5.64 a	44.99 ± 2.90 a	36.04 ± 2.41 b
Stage 5	94.48 ± 3.59 b	78.51 ± 3.80 b	42.87 ± 4.38 b	29.20 ± 3.30 b	86.29 ± 4.59 a
Stage 6	46.82 ± 3.76 d	50.18 ± 2.77 c	28.70 ± 3.14 c	17.53 ± 0.94 c	89.01 ± 4.46 a
Significant	**	**	**	**	**
CV	10.42	10.44	16.69	16.01	11.74
LSD (<i>P</i> < 0.05)	12.92	17.78	11.46	7.61	9.38

Table 2. SOD, CAT, APX and GR activity accompanying by endogenous H₂O₂ accumulation during rose flowers development from bud opening to petal senescence. Data shown are mean values of *n* = 3, and the error bars represent standard errors of the means. Mean values followed by different letters indicate they are different by LSD test at *P* < 0.05.

cence, thus extending vase life in cut rose flowers. Matching with higher *SUMO1* and *SUMO E3 ligase SIZ1* genes expression, the lower endogenous H₂O₂ accumulation (Fig. 3A; *P* < 0.01) in cut rose flowers after the administration of 150 nM PSK α treatment might be attributed to higher expression and activities of SOD, CAT, APX, and GR (Table 5; *P* < 0.01). As shown in Fig. 3B, higher endogenous proline accumulation (*P* < 0.01) in cut rose flowers following the administration of 150 nM PSK α treatment might be attributed to higher expression and activities of *P5CS* and *OAT* (Table 6; *P* < 0.01). Furthermore, 150 nM PSK α treatment promoted GABA utilizing (Fig. 3C) by the activity of GABA shunt pathway as realized by higher expression and activities of *GAD*, *GABA-T*, and *SSADH* (Table 7; *P* < 0.01) in cut rose flowers. Moreover, higher expression of *HSP70* and *HSP90* (Fig. 4A,B; *P* < 0.01) in cut rose flowers following the administration of 150 nM PSK α treatment might be accountable for postponing senescence (Supplementary Fig. 1).

Discussion

During rose flower bud opening, glucose supply from light and CO₂ dependent photosynthesis might be accountable for increasing TOR signaling pathway by providing energy relay through glycolysis pathway, tricarboxylic acid cycle, and electron transporting system³⁷. In addition, providing sulfide (S₂⁻) from sulfate (SO₄²⁻) assimilation mediated by sulfite reductase (SiR) enzyme might be accountable for increasing TOR signaling pathway by increasing glucose supply and promoting the activity of the glucose/energy signaling pathway³⁸. In addition,

Flower development stages	P5CS activity (U kg ⁻¹)	OAT activity (U kg ⁻¹)	Proline accumulation (mmol kg ⁻¹ FW)
Stage 1	11.93 ± 0.81 c	8.25 ± 0.61 d	15.46 ± 0.34 e
Stage 2	15.37 ± 1.42 bc	11.28 ± 0.93 d	26.57 ± 1.55 d
Stage 3	22.33 ± 1.84 b	13.27 ± 0.49 cd	38.97 ± 3.40 c
Stage 4	38.97 ± 3.82 a	17.26 ± 1.15 c	55.86 ± 3.59 b
Stage 5	38.62 ± 3.83 a	39.32 ± 3.19 a	69.13 ± 4.79 a
Stage 6	33.07 ± 2.21 a	32.64 ± 1.96 b	54.51 ± 2.70 b
Significant	**	**	**
CV	16.79	14.24	12.31
LSD (<i>P</i> < 0.05)	7.98	5.15	9.51

Table 3. P5CS and OAT activity accompanying by proline accumulation during rose flowers development from bud opening to petal senescence. Data shown are mean values of *n* = 3, and the error bars represent standard errors of the means. Mean values followed by different letters indicate they are different by LSD test at *P* < 0.05.

Flower development stages	GAD activity (μmol kg ⁻¹ min ⁻¹)	GABA-T activity (μmol kg ⁻¹ min ⁻¹)	SSADH activity (μmol kg ⁻¹ min ⁻¹)	GABA accumulation (mmol kg ⁻¹ FW)
Stage 1	25.86 ± 2.34 d	19.26 ± 1.40 d	9.26 ± 0.74 e	18.53 ± 0.56 d
Stage 2	38.52 ± 3.29 bc	22.46 ± 1.58 cd	13.51 ± 0.87 de	22.46 ± 1.55 cd
Stage 3	55.16 ± 2.95 a	27.41 ± 2.08 bc	17.43 ± 1.29 cd	29.08 ± 3.73 bc
Stage 4	60.14 ± 4.79 a	24.37 ± 1.29 cd	22.71 ± 1.54 c	39.56 ± 3.96 a
Stage 5	42.84 ± 1.82 b	31.24 ± 2.53 b	33.21 ± 1.94 b	33.05 ± 1.90 ab
Stage 6	29.52 ± 2.31 cd	49.45 ± 3.54 a	42.69 ± 3.92 a	28.88 ± 2.40 bc
Significant	**	**	**	**
CV	12.66	13.20	15.13	15.95
LSD (<i>P</i> < 0.05)	9.46	6.81	6.23	8.11

Table 4. GAD, GABA-T and SSADH activity accompanying by GABA accumulation during rose flowers development from bud opening to petal senescence. Data shown are mean values of *n* = 3, and the error bars represent standard errors of the means. Mean values followed by different letters indicate they are different by LSD test at *P* < 0.05.

glucose and light-dependent auxin biosynthesis may trigger the TOR signaling pathway by activating ROP2 GTPase³⁹. In addition to glucose and light-dependent auxin biosynthesis, ROP2 GTPase might be activated by sufficient nitrate (NO₃⁻) and ammonium (NH₄⁺) to trigger TOR signaling pathway. In addition, providing glutamine (Gln) from nitrogen assimilation, delivering cysteine (Cys) from sulfur assimilation, and providing glycine (Gly) from the glycolate pathway exhibit the highest potency for increasing TOR signaling pathway by activating ROP2 GTPase^{40–42}. Moreover, increasing glucose supply and promoting the activity of the glucose/energy signaling pathway is not accountable for increasing TOR signaling pathway following nitrate-ammonium supplying^{40–42}. In plants, the TOR signaling pathway might be accountable for increasing plant growth-promoting auxin (IAA), gibberellic acid (GA3), brassinosteroids (BRs), and cytokinins (CKs) signaling while suppressing plant growth-inhibiting abscisic acid (ABA), jasmonic acid (JA), salicylic acid (SA), and ethylene (ETH) signaling⁴². By activating endogenous GA3 biosynthesis and signaling from the TOR signaling pathway, petal cell expansion, hypertrophy, or enlargement is promoted by the accumulation of vacuolar sugars, cell wall loosening or relaxation, and vacuolar water flows^{43,44}. In addition, promoting the degradation of starch and sucrose through the TOR signaling pathway might be accountable for the greater decorative quality of rose flowers during bud opening because it provides sufficient intracellular glucose 6-phosphate used to supply sufficient intracellular (1) ATP through glycolysis pathway, tricarboxylic acid cycle, and electron transporting system, and (2) NADPH, erythritol-4-phosphate, and ribose 5-phosphate through oxidative pentose phosphate pathway^{37,43,44}. Following the exogenous supply of glucose, the increase of SUMO1/2 accumulation and *SUMO E3 ligase SIZ1* gene expression demonstrated that the SUMOylation might be activated by providing exogenous glucose for the activation of transcription factors. SUMO E3 ligase SIZ1 is accountable for preserving the stability and promoting the transcriptional activity of transcription factors by their SUMOylation and by suppressing their degradation by ubiquitin–proteasome system. Therefore, following the exogenous supplying of glucose or providing endogenous glucose, TOR signaling might be accountable for increasing the activity of SUMO E3 ligase SIZ1, thus suppressing the SnRK1 signaling pathway^{8,45}. Therefore, it can be assumed that promoting the glucose-TOR signaling pathway might increase the SUMO1/SUMO E3 ligase SIZ1 signaling pathway in rose flowers during bud opening. Therefore, the greater decorative quality of flowers might be attributed to SUMO1/

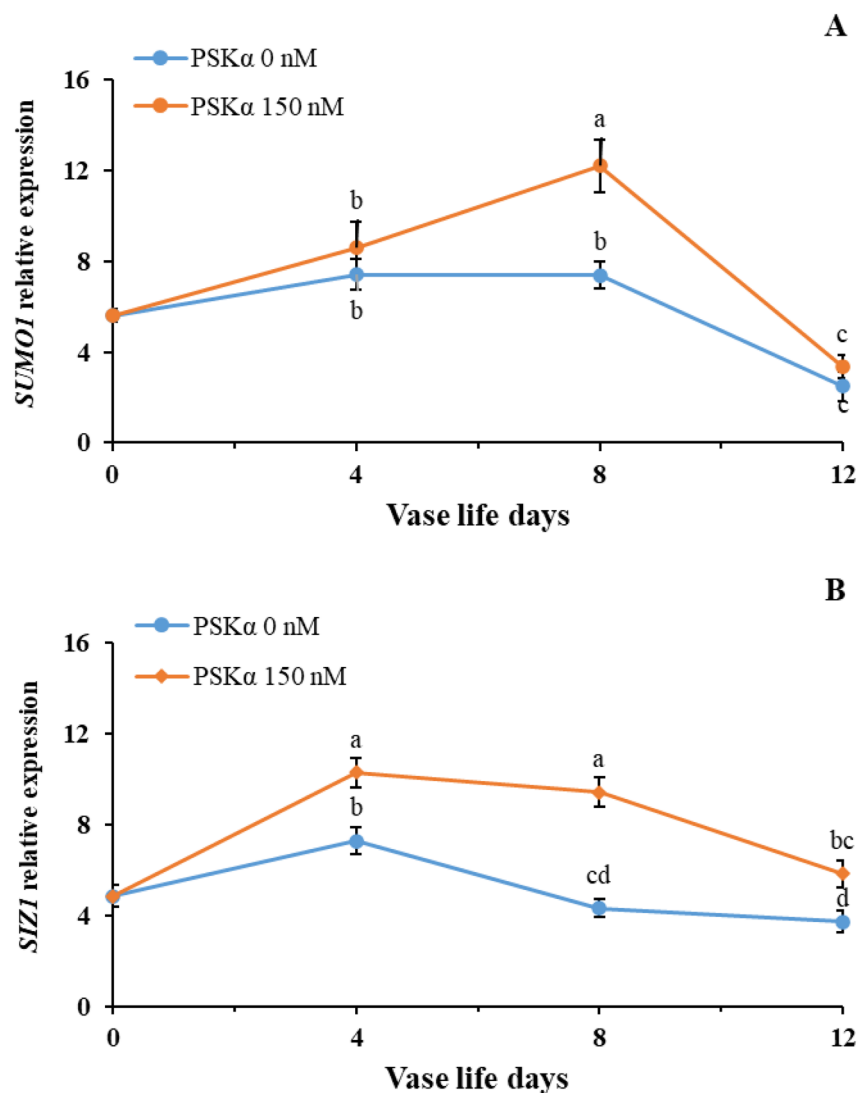


Figure 2. *SUMO1* (A) and *SUMO E3 ligase SIZ1* (B) genes expression in petals of rose flowers treated with PSK α at 0 and 150 nM during vase life at 20 °C for 12 days. Data shown are mean values of $n=3$, and the error bars represent standard errors of the means. Mean values followed by different letters indicate they are different by LSD test at $P<0.05$.

SUMO E3 ligase SIZ1 signaling pathway achieved from the glucose-TOR signaling pathway. Following harvest, the suppression of the glucose-TOR signaling pathway in cut rose flowers might be accountable for deactivating the SUMO1/SUMO E3 ligase SIZ1 signaling pathway during vase life. Therefore, the lower decorative quality of cut rose flowers during vase life might be attributed to the lower activity of the SUMO1/SUMO E3 ligase SIZ1 signaling pathway that is achieved from the suppression of the glucose-TOR signaling pathway.

In plants, SUMO E3 ligase SIZ1 is accountable for SUMOylation of ICE1 transcription factor, suppressing poly-ubiquitination of ICE1 by E3 ubiquitin ligase HOS1 stabilizing ICE1⁴. In addition, SUMO-ICE1 inhibited MYB15 as a repressor of CBF3/COR expression. SUMOylation of ICE1 by SUMO E3 ligase SIZ1 promotes the CBF3 signaling pathway directly by ICE1 transcriptional activity or indirectly by suppressing MYB15 transcriptional activity⁴. The binding of CBFs to CRT/DRE motif in promoter of *CORs* genes (1) enhances the activity of ROS scavenging systems, (2) ensures a sufficient intracellular supply of ATP, (3) promotes *HSPs* gene expression, and (4) activates the endogenous accumulation of polyamines, proline, and GABA by promoting the activity of arginine pathways⁴⁶. In plants, SUMO E3 ligase SIZ1 dependent SUMOylation enhances the activity of NR enzyme and preserves NR protein stability, which not only improves the activity of glutamine synthetase/glutamate synthase (GS/GOGAT) cycle by supplying NH_4^+ but also activates the endogenous accumulation of nitric oxide¹⁰. SUMO E3 ligase SIZ1 is accountable for SUMOylation of MYB75 and MYB1 transcription factors, which improves their stability for increasing the expression of phenylpropanoid pathway for promoting the accumulation of anthocyanins^{13,14}. In addition to anthocyanin accumulation, the supplying of NH_4^+ through the activity of phenylalanine ammonia-lyase (PAL) enzyme might be accountable for providing glutamate via GS/GOGAT cycle⁴⁷. In plants, the activity of the NR enzyme is accountable for producing NO_2^- for the activity

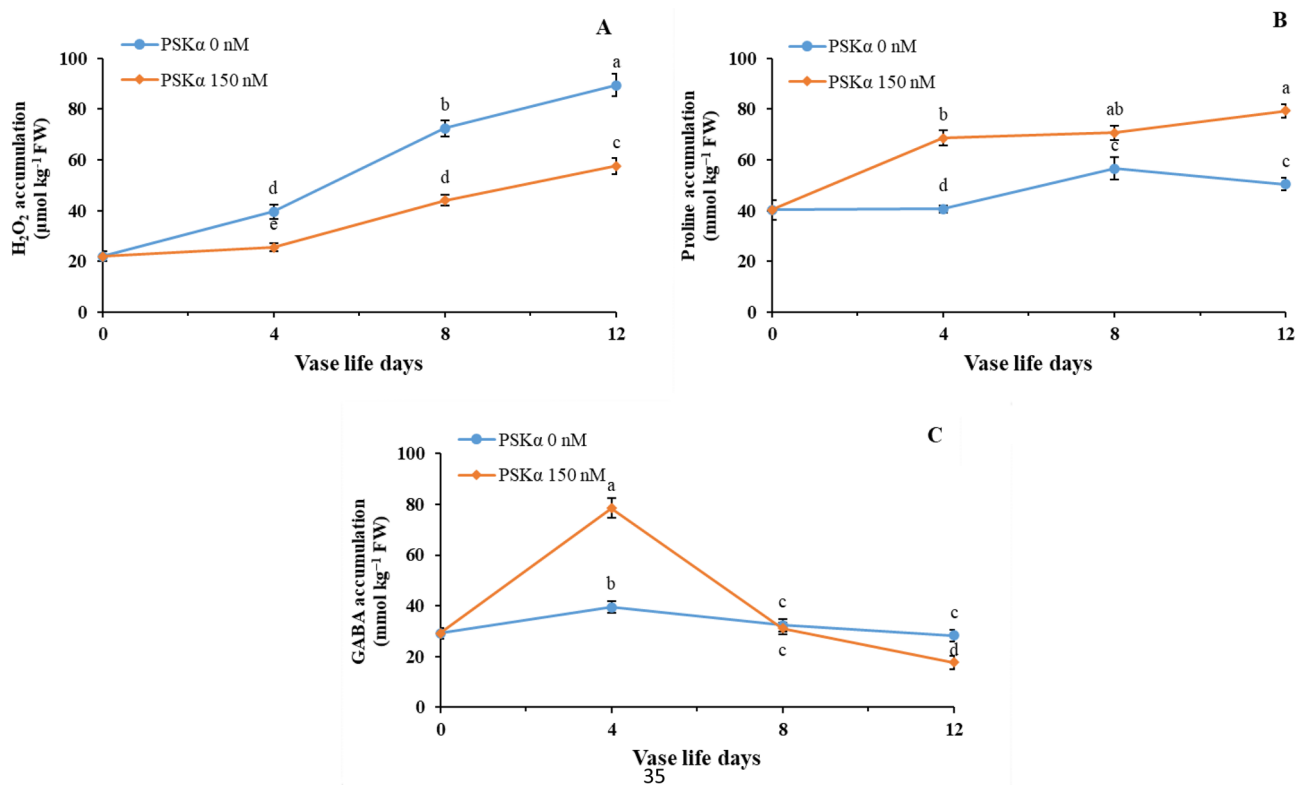


Figure 3. Endogenous H₂O₂ (A), proline (B) and GABA (C) accumulation in petals of rose flowers treated with PSKα at 0 and 150 nM during vase life at 20 °C for 12 days. Data shown are mean values of n = 3, and the error bars represent standard errors of the means. Mean values followed by different letters indicate they are different by LSD test at P < 0.05.

PSKα treatment (nM)	Vase life (days)	Genes relative expression				Enzyme's activity (U kg ⁻¹)			
		SOD	CAT	APX	GR	SOD	CAT	APX	GR
0	0	6.37 ± 0.85	7.23 ± 0.57	3.78 ± 0.34	3.25 ± 0.29	58.60 ± 4.36	128.73 ± 5.40	49.42 ± 4.85	37.52 ± 6.26
	4	8.66 ± 0.71 bc	5.95 ± 0.52 cd	8.67 ± 0.38 bc	6.51 ± 0.41 b	85.58 ± 2.5 b	110.53 ± 2.67 b	72.35 ± 2.33 c	42.38 ± 2.42 b
	8	8.31 ± 0.64 bc	7.41 ± 0.80 c	7.34 ± 0.52 cd	8.16 ± 0.66 b	72.26 ± 1.14 c	72.26 ± 2.42 d	39.55 ± 1.84 e	33.25 ± 1.67 c
	12	3.47 ± 0.27 d	2.87 ± 0.39 e	5.54 ± 0.61 d	3.65 ± 0.28 c	36.23 ± 1.09 e	29.90 ± 1.77 e	28.35 ± 1.29 f	16.22 ± 0.91 d
150	4	10.39 ± 0.98 ab	10.32 ± 0.66 b	12.33 ± 1.11 a	7.28 ± 0.49 b	98.56 ± 4.10 a	136.55 ± 5.07 a	95.45 ± 2.67 a	48.15 ± 3.40 ab
	8	12.30 ± 1.63 a	13.74 ± 1.41 a	10.60 ± 0.79 ab	11.39 ± 1.28 a	103.09 ± 4.14 a	98.87 ± 4.79 c	82.55 ± 3.54 b	52.61 ± 3.95 a
	12	6.52 ± 0.47 c	4.85 ± 0.27 de	6.33 ± 0.34 d	8.45 ± 0.62 b	59.70 ± 1.89 d	39.49 ± 2.45 e	47.49 ± 1.65 d	40.43 ± 2.65 bc
Significant	df								
Treatment	1	**	**	**	**	**	**	**	**
Time	2	**	**	**	**	**	**	**	**
T × T	2	ns	*	ns	*	*	*	**	*
CV	-	18.81	17.70	13.86	16.01	6.35	7.31	6.64	12.02
LSD (P = 0.05)		2.77	2.37	2.09	2.16	8.57	10.58	7.21	8.31

Table 5. SOD, CAT, APX and GR genes expression and enzymes activity in petals of rose flowers treated with PSKα at 0 and 150 nM during vase life at 20 °C for 12 days. Data shown are mean values of n = 3, and the error bars represent standard errors of the means. Mean values followed by different letters indicate they are different by LSD test at P < 0.05.

PSKa treatment (nM)	Vase life (days)	Genes relative expression		Enzyme's activity ($\mu\text{mol kg}^{-1} \text{min}^{-1}$)	
		P5CS	OAT	P5CS	OAT
0	0	5.83 ± 0.57	3.80 ± 0.49	22.82 ± 1.23	13.57 ± 1.40
	4	8.42 ± 1.02 b	3.97 ± 0.37 c	25.33 ± 1.76 c	15.21 ± 0.62 d
	8	9.58 ± 0.83 b	4.61 ± 0.36 c	37.85 ± 2.97 b	38.41 ± 0.98 b
	12	3.63 ± 1.38 c	7.45 ± 0.70 b	12.36 ± 1.04 d	15.73 ± 0.65 d
150	4	14.48 ± 1.56 a	7.57 ± 0.52 b	42.69 ± 2.45 b	22.13 ± 1.08 c
	8	15.52 ± 1.79 a	10.47 ± 0.58 a	74.47 ± 3.18 a	55.05 ± 2.92 a
	12	9.50 ± 0.73 b	9.66 ± 0.60 a	39.30 ± 2.46 b	39.54 ± 1.60 b
Significant	df				
Treatment	1	**	**	**	**
Time	2	**	**	**	**
T × T	2	ns	*	**	**
CV	-	21.76	12.79	10.85	8.54
LSD ($P=0.05$)		3.94	1.66	7.46	4.71

Table 6. P5CS and OAT genes expression and enzymes activity in petals of rose flowers treated with PSKa at 0 and 150 nM during vase life at 20 °C for 12 days. Data shown are mean values of $n=3$, and the error bars represent standard errors of the means. Mean values followed by different letters indicate they are different by LSD test at $P<0.05$.

PSKa treatment (nM)	Vase life (days)	Genes relative expression			Enzyme's activity ($\mu\text{mol kg}^{-1} \text{min}^{-1}$)		
		GAD	GABA-T	SSADH	GAD	GABA-T	SSADH
0	0	4.26 ± 0.28	3.57 ± 0.34	2.96 ± 0.31	54.67 ± 4.42	27.48 ± 1.46	17.20 ± 1.21
	4	10.04 ± 0.61 b	3.98 ± 0.25 d	4.34 ± 0.14 c	59.26 ± 3.60 b	30.78 ± 1.54 c	21.46 ± 0.65 d
	8	5.33 ± 0.62 cd	5.32 ± 0.35 c	7.50 ± 0.27 b	42.35 ± 1.32 c	32.29 ± 1.65 c	32.37 ± 1.61 c
	12	2.64 ± 0.18 d	6.61 ± 0.35 b	8.55 ± 0.26 b	29.38 ± 0.97 d	51.73 ± 0.94 ab	42.69 ± 1.66 b
150	4	16.19 ± 1.74 a	4.28 ± 0.16 d	5.28 ± 0.21 c	67.69 ± 1.92 a	35.37 ± 1.61 c	26.39 ± 0.78 d
	8	7.74 ± 0.75 bc	7.41 ± 0.34 b	10.77 ± 0.88 a	62.66 ± 1.51 ab	46.98 ± 1.74 b	46.69 ± 2.24 b
	12	3.52 ± 0.83 d	10.39 ± 0.44 a	11.83 ± 0.64 a	48.89 ± 3.40 c	57.62 ± 3.25 a	54.07 ± 2.30 a
Significant	df						
Treatment	1	**	**	**	**	**	**
Time	2	**	**	**	**	**	**
T × T	2	*	**	*	*	*	*
CV	-	21.01	9.00	10.36	7.88	7.84	7.75
LSD ($P=0.05$)			1.01	1.48	7.25	5.92	5.14

Table 7. GAD, GABA-T and SSADH genes expression and enzymes activity in petals of rose flowers treated with PSKa at 0 and 150 nM during vase life at 20 °C for 12 days. Data shown are mean values of $n=3$, and the error bars represent standard errors of the means. Mean values followed by different letters indicate they are different by LSD test at $P<0.05$.

of nitrite reductase enzyme for supplying NH_4^+ . In chloroplast or mitochondria, the GS enzyme is accountable for providing glutamine from glutamate and NH_4^+ . With the activity of the GOGAT enzyme, two glutamate molecules are produced from α -ketoglutarate, and one glutamate molecule is essential for allowing GS/GOGAT cycle to continue. With the activity of the GS/GOGAT cycle, glutamate supply is useful for proline and GABA biosynthesis. In addition, a sufficient intracellular supply of glutamate might be accountable for arginine supplying for starting the activity of the ARG/NOS pathway for the endogenous accumulation of nitric oxide, polyamines, proline, and GABA^{48,49}. Therefore, SUMO E3 ligase SIZ1 may increase glutamate supply by promoting the activity of NR/PAL enzymes. The glutamate supply is used by ICE1/CBFs signaling pathway for supporting the biosynthesis proline and GABA. In plants, a sufficient glutamate supply provided by GS/GOGAT cycle might be accountable for proline biosynthesis by the P5CS enzyme. In addition to glutamate, the delivery of ornithine is responsible for proline biosynthesis by the OAT enzyme^{48,50}. Endogenous proline serves as an osmoprotectant and exhibits ROS scavenging capacity, which is beneficial for keeping membrane integrity and is also helping as a chaperoning molecule for stabilizing ROS scavenging proteins⁴⁸. In addition to proline, the glutamate supply provided by GS/GOGAT cycle might be accountable for GABA biosynthesis through the activity of the GAD enzyme⁵¹. In addition to osmoregulation capacity, the endogenous GABA, as an osmoprotectant, exhibits ROS scavenging capacity.

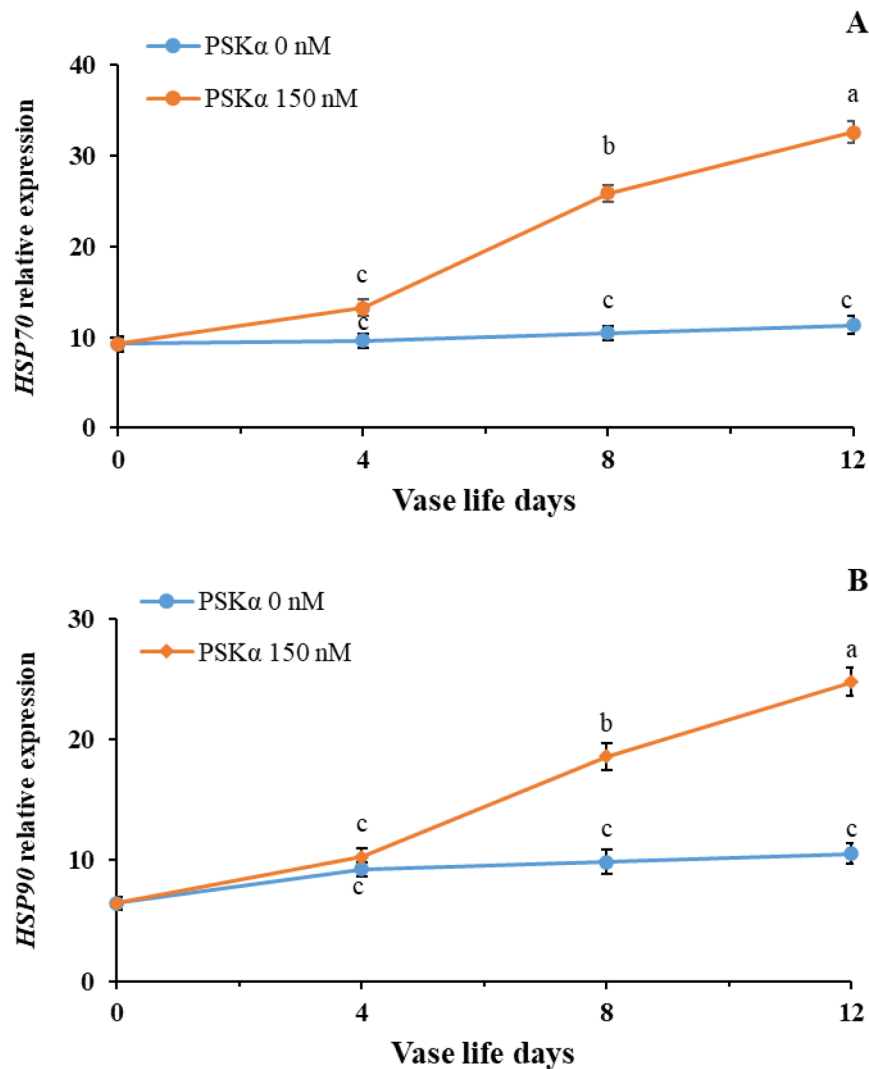


Figure 4. *HSP70* (A) and *HSP90* (B) genes expression in petals of rose flowers treated with PSKα at 0 and 150 nM during vase life at 20 °C for 12 days. Data shown are mean values of n=3, and the error bars represent standard errors of the means. Mean values followed by different letters indicate they are different by LSD test at $P < 0.05$.

Furthermore, endogenous GABA accumulation by the GAD enzyme prevents cytosolic acidification during senescence and stress⁵². In our study, increasing the activity of ICE1/CBFs transcriptional system accompanied by ensuring a sufficient supply of glutamate through GS/GOGAT cycle by SUMO1/SUMO E3 ligase SIZ1 signaling pathway might be accountable for activating endogenous accumulation of proline and GABA in rose flowers during bud opening, achieving from higher expression and activity of *P5CS* and *GAD*, respectively. Therefore, the superior decorative quality of rose flowers during bud opening might be attributed to the higher endogenous proline and GABA accumulation accompanied by promoting SUMO1/SUMO E3 ligase SIZ1 signaling pathway.

In plants, unfriendly ROS accumulation accelerates the deterioration of membrane integrity by increasing the peroxidation of membrane unsaturated fatty acids as realized by a higher MDA accumulation. For countering oxidative stress, plants have evolved ROS-avoiding and scavenging systems⁵². In plants, SUMOylation as a molecular switch is accountable for maintaining intracellular ROS homeostasis. SUMO E3 ligase SIZ1 is accountable for intracellular ROS homeostasis by increasing expression of alternative oxidase (*AOX*) and uncoupling protein 1 (*UCP1*) genes, which is a ROS avoidance strategy, which also promotes gene expression and expression and activities of ROS scavenging *SOD*, *CAT*, *APX*, and *GR*. In addition, by suppressing endogenous salicylic acid biosynthesis through the isochorismate synthase pathway, SUMO E3 ligase SIZ1 may prevent ROS accumulation by stopping NADPH oxidases^{8,11,12}. Mishra et al.⁵³ reported that the rice *SUMO E3 ligase SIZ1* gene overexpression conferred heat and drought stress tolerance in cotton plants by improving photosynthesis performance by protecting the activity of the electron transport system, increasing *HSPs* expression, and promoting *SOD* and *APX* expression. Zhang et al.⁵⁴ reported that the tomato *SUMO E3 ligase SIZ1* gene overexpression conferred drought tolerance in tobacco by activating endogenous accumulation of proline achieving from higher *P5CS* gene expression, lower accumulation of O_2^- and H_2O_2 achieving from higher expression and activity of *CAT* and

APX, suppressing chlorophyll degradation and preserving leaf water status, and maintaining membrane integrity as realized by lower MDA accumulation. Zhang et al.⁷ reported that the SUMO E3 ligase *SIZ1* gene overexpression conferred heat tolerance while SUMO E3 ligase *SIZ1* gene silencing by RNA interference aggregated heat damage in the tomato plants. During heat stress, *SIZ1* is accountable for HSFs SUMOylation for increasing *HSP70* and *HSP90* expression. Moreover, *SIZ1* might be responsible for stabilizing *HSP70* and *APX* proteins through their SUMOylation. With SUMO E3 ligase *SIZ1* gene overexpression, the preservation of membrane integrity as realized by lower MDA accumulation might be attributed to higher endogenous proline accumulation achieved from higher *P5CS* gene expression, higher expression of molecular chaperones *HSP70* and *HSP90* and the accumulation of their proteins, and lower accumulation of O_2^- and H_2O_2 achieved from higher *APX* expression and activity⁷. In our study, a sufficient sugar supply in rose flowers during bud opening promotes the glucose-TOR signaling pathway. Then, the activation of SUMO1/SUMO E3 ligase *SIZ1* signaling pathway by glucose-TOR signaling pathway employed ICE1/CBFs and HSFs/HSPs transcriptional signaling systems. In plants, ICE1/CBFs and HSFs/HSPs transcriptional activity might be accountable for attenuating endogenous H_2O_2 accumulation by promoting ROS scavenging *SOD*, *CAT*, *APX*, and *GR* expression and activity, leading to lower MDA accumulation^{55–58}. Therefore, the superior decorative quality of rose flowers during bud opening might be attributed to higher ROS scavenging *SOD*, *CAT*, *APX*, and *GR* expression and activity associated with activating SUMO1/SUMO E3 ligase *SIZ1* signaling pathway.

After flowers are harvested, the suppression of the TOR signaling pathway and promoting the SnRK1 signaling pathway by intracellular deficiency of sugar and water stress accelerate petal senescence due to intracellular insufficiency of ATP and NADPH supply and unfriendly intracellular accumulation of ROS. The SnRK1 signaling pathway employs bZIPs transcription factors for orchestrating intracellular sugar and energy homeostasis by intracellular ATP shortage. After flowers are harvested, insufficient sugar supply in rose flowers during petal senescence suppresses the glucose-TOR signaling pathway. By stopping the glucose-TOR signaling pathway, the SnRK1 signaling pathway's increased activity might be accountable for suppressing SUMO1/SUMO E3 ligase *SIZ1* signaling pathway in rose flowers during petal senescence. In plants, ICE1/CBFs and HSFs/HSPs transcriptional activity might be accountable for attenuating endogenous H_2O_2 accumulation by promoting gene expression and activities of ROS scavenging *SOD*, *CAT*, *APX*, and *GR*. In our study, higher endogenous H_2O_2 accumulation arising from lower gene expression and activities of ROS scavenging *SOD*, *CAT*, *APX*, and *GR* in rose flowers during petal senescence was associated with lower *SUMO1* and *SUMO E3 ligase SIZ1* genes expression. As a result, the inferior decorative quality of rose flowers might be attributed to the lower activity of the ROS scavenging system accompanied by the lower SUMO1/SUMO E3 ligase *SIZ1* signaling pathway.

In rose flowers during petal senescence, the lower *SUMO1* and *SUMO E3 ligase SIZ1* genes expression was associated with lower *P5CS* expression and activity. Higher *OAT* expression and activity might be responsible for proline accumulation in rose flowers during petal senescence. Kumar et al.⁵⁹ reported that the higher activity of the *P5CS* enzyme is responsible for endogenous proline accumulation in rose flowers during bud opening. The activity of the *GS* enzyme is accountable for providing the *P5CS* enzyme with glutamate. However, lower activity of *GS* enzyme was concomitant with higher activity of *NADH-GDH* enzyme, beneficial for the activity of glutamate supplying *P5CS* and for the detoxification of NH_4^+ produced by proteolysis during rose flower senescence. The higher NH_4^+ accumulation from the higher proteolysis may serve as a signal for promoting the activity of the *NADH-GDH* enzyme during rose flower senescence.

Additionally, the higher activity of the *OAT* enzyme under water deficiency might be accountable for proline biosynthesis from ornithine during rose flower senescence. With the supply of ornithine from proteolysis through the urea cycle during rose flower senescence, supplying one molecule NADPH for pyrroline-5-carboxylate reductase (*P5CR*) is accountable for proline biosynthesis, whereas providing of one molecule ATP and two molecules NADPH is accountable for proline biosynthesis from glutamate. Therefore, *OAT* enzyme activity might be responsible for proline biosynthesis from ornithine during rose flower senescence by insufficient intracellular ATP provision accompanied by water deficiency⁵⁹. Therefore, a sufficient endogenous supply of proline by *OAT* expression and activity during petal senescence in rose flowers might be provided by the proline dehydrogenase (*ProDH*) enzyme for a sufficient intracellular provision of ATP accompanied by friendly ROS accumulation. In plants, activities of ICE1/CBFs and NR/MYBs pathways might be accountable for endogenous proline accumulation by increasing *P5CS* gene expression and enzyme activity along with sufficient intracellular supply of glutamate. In our study, higher endogenous proline accumulation accompanied by lower SUMO1/SUMO E3 ligase *SIZ1* signaling pathway in rose flowers during petal senescence might be attributed to higher *OAT* expression and activity. As a result, the inferior decorative quality of rose flowers might be attributed to lower glutamate supply for proline biosynthesis due to lower *P5CS* expression and activity, which was accompanied by lower *SUMO1* and *SUMO E3 ligase SIZ1* genes expression.

In rose flowers during petal senescence, lower *SUMO1* and *SUMO E3 ligase SIZ1* genes expression was associated with lower endogenous GABA accumulation achieved from the higher activity of GABA shunt pathway realized by *GABA-T* and *SSADH* expression and activity. In rose flowers during petal senescence, promoting the activity of GABA shunt pathway might be accountable for allowing the activity of tricarboxylic acid cycle by providing succinate through the activity of *SSADH* enzyme, leading to sufficient supply of NADH and carbon skeletons. Moreover, the delivery of NADH and succinate by the *SSADH* enzyme might be accountable for the activity of the mitochondria electron-transporting system, providing a sufficient ATP supply and avoiding ROS accumulation^{51,60,61}. In plants, for protein succinylation, the tricarboxylic acid cycle is crucial as it supplies succinate or succinyl-CoA. During rose flower petal senescence, lower activities of α -ketoglutarate dehydrogenase and succinyl-CoA synthetase enzymes in the tricarboxylic acid cycle led to unfriendly ROS accumulation, which may restrict succinate supply for protein succinylation. Hence, the GABA shunt pathway might be crucial for succinate for succinylation of the tricarboxylic acid cycle and electron transporting system proteins, which is beneficial for supporting a sufficient ATP supply and ROS signaling⁶². With the activity of the GABA shunt

pathway, providing sufficient succinate for succinylation is crucial for the glycolysis pathway, tricarboxylic acid cycle, and electron transport system activity for higher ATP supply and lower ROS accumulation which might be beneficial for postponing rose flower petal senescence^{63,64}. In plants, ICE1/CBFs and NR/MYBs pathways might be accountable for (1) endogenous accumulation of GABA by increasing *GAD* gene expression and enzyme activity and (2) sufficient intracellular supply of glutamate. In our study, lower endogenous GABA accumulation associated with lower SUMO1/SUMO E3 ligase SIZ1 signaling pathway in rose flowers during petal senescence might be attributed to the higher activity of the GABA shunt pathway by increasing *GABA-T* and *SSADH* expression and activity. As a result, the inferior decorative quality of rose flowers might be attributed to lower glutamate supply for GABA biosynthesis due to lower *GAD* expression and activity, which was accompanied by lower *SUMO1* and *SUMO E3 ligase SIZ1* genes expression. Therefore, a sufficient endogenous GABA supply by *GAD* expression and activity during bud opening in rose flowers might be utilized by *GABA-T* and *SSADH* expression and activity, which is required for intracellular ATP provision and avoiding ROS accumulation in rose flowers during petal senescence.

By serving as a moonlighting protein, the PSK α receptor (PSKR1) exhibits protein kinase and guanylate cyclase activity. Following the administration of PSK α treatment, the cytosolic accumulation of cGMP, the activation of protein kinase G (PKG), and cyclic nucleotide-gated ion channel (CNGC) could be responsible for PSK α signal transduction^{65,66}. Aghdam et al.¹⁷ reported that the PSK α treatment at 150 nM extended the vase life of cut rose flowers due to the cytosolic accumulation of cGMP, which promoted PKG and CNGC1 expression, thus realizing activated PSK α signal transduction for postponing petal senescence. Following the application of 150 nM PSK α , the reinforcement of the endogenous PSK α signaling pathway by suppressing phosphodiesterase (*PDE*) gene expression might be accountable for postponing senescence and extending the vase life of cut rose flowers¹.

The translocation of HSFs from the cytoplasm to the nucleus is crucial for HSFs binding to heat shock elements (HSEs) in HSPs gene promoters for increasing the expression of HSPs. In addition, HSFs may serve as cellular redox sensors by activating *APX* gene expression for ROS scavenging during senescence⁵⁶. In our study, following the application of 150 nM PSK α treatment, increasing HSFs/HSPs transcriptional activity by SUMO1/SUMO E3 ligase SIZ1 signaling pathway might not only be accountable for increasing the expression of *HSP70* and *HSP90* but might also be accountable for enhancing the activity of ROS scavenging system in cut rose flowers during vase life. *HSPs* expression and protein accumulation serve as intracellular molecular chaperones beneficial for protein synthesis, renaturation, and stabilization. *HSPs* migration from the cytosol to the membrane during senescence and stress is crucial for keeping membranes integrity and fluidity. In addition, *HSPs* exhibit ROS scavenging capacity beneficial for keeping membranes fluidity and integrity by protecting fatty acids against peroxidation by ROS accumulation during senescence and stress. In addition, the binding of *HSPs* to membrane phospholipids and galactolipids is beneficial for keeping membranes fluidity and integrity. By binding to the membrane phospholipids and galactolipids, *HSPs* preserve membranes integrity by blocking the binding of phospholipase enzymes to membranes. Furthermore, *HSPs* are crucial for keeping the stability of mitochondrial and chloroplast electron-transporting proteins beneficial for providing a sufficient intracellular supply of ATP and avoiding ROS accumulation. *HSPs* are useful for intensifying intracellular ROS scavenging capacity by promoting the accumulation of ROS scavenging AA and GSH molecules and the activities of ROS scavenging enzymes^{55,56,67,68}. In addition, Gagné et al.⁶⁹ reported that the PARP1 suppresses *HSP70* gene expression by binding to the *HSP70* promoter. By heat stress sensing, SUMO E3 ligase SIZ1 and SUMO E4 ligase are accountable for PARP1 polySUMOylation, which targets PARP1 for ubiquitination by ubiquitin E4 ligases for PARP1 degradation by the ubiquitin–proteasome system. With the degradation of PARP1, PARP1 clearance from the *HSP70* promoter contributes to *HSP70* gene expression. Therefore, SUMOylation by SUMO E3 ligase SIZ1 might be accountable for regulating the expression of *HSPs*⁷⁰. With the suppression of *PARP1* gene expression following the application of PSK α treatment²¹, the higher activity of the SUMO1/SUMO E3 ligase SIZ1 signaling pathway might be accountable for increasing the expression of *HSP70* and *HSP90* in cut rose flowers during the vase life. Therefore, the superior decorative quality of rose flowers following the 150 nM PSK α treatment application might be attributed to higher expression of *HSP70* and *HSP90* achieved from SUMO1/SUMO E3 ligase SIZ1 signaling pathway. In our study, associated with higher *SUMO1* and *SUMO E3 ligase SIZ1* genes expression, higher expression of *HSP70* and *HSP90* in cut rose flowers during vase life might be accountable for postponing petal senescence.

Developmental factors and hormonal cues such as gibberellin and cytokinin^{71–73}, brassinosteroids or ERFs transcriptional activity^{74,75} during bud opening may be responsible for triggering *PSKs* genes expression¹. By triggering PSK α signaling, promoting PKG, Ca²⁺/CaM or CDPK may be responsible for cytosolic cGMP signal responsive genes expression¹. Transcription factors stability, DNA binding capacity, and subcellular location orchestration directly by PKG, Ca²⁺/CaM, or CDPK⁷⁶ or indirectly by SUMO1/SIZ1 signaling pathway⁷⁷ may be responsible for ROS scavenging, along with proline, and GABA biosynthesis responsive genes expression. In addition, SUMO1/SIZ1 signaling pathway may serve as a downstream target of PSK α signaling for ROS scavenging, proline, and GABA biosynthesis responsive proteins SUMOylation^{4,7–9,12,78–80} which could support flower decorative quality by maintaining intracellular energy and ROS homeostasis^{81–84}. By flower harvesting, developmental factors and hormonal cues such as ABA and ethylene (water shortage stress)^{71–73,84} may be responsible for suppressing PSK α signaling by triggering *PDE* gene expression for preventing cytosolic cGMP signaling or repressing *PSKs* genes expression¹. By suppressing PSK α signaling, impeding PKG, Ca²⁺/CaM, or CDPK and/or SUMO1/SIZ1 signaling pathway may confine ROS scavenging system activity and proline and GABA biosynthesis. Consequently, disrupting intracellular energy and ROS homeostasis^{81,82,84} may be responsible for decorative quality losing and vase life termination of flowers. Therefore, unfriendly intracellular ROS accumulation and insufficient intracellular ATP supply, probably resulting from confined PKG, Ca²⁺/CaM, or CDPK and/or SUMO1/SIZ1 signaling pathway, are intrinsic features of petals senescence. In addition, reinforcing endogenous PSK α signaling associated with promoting SUMO1/SIZ1 signaling pathway could be responsible

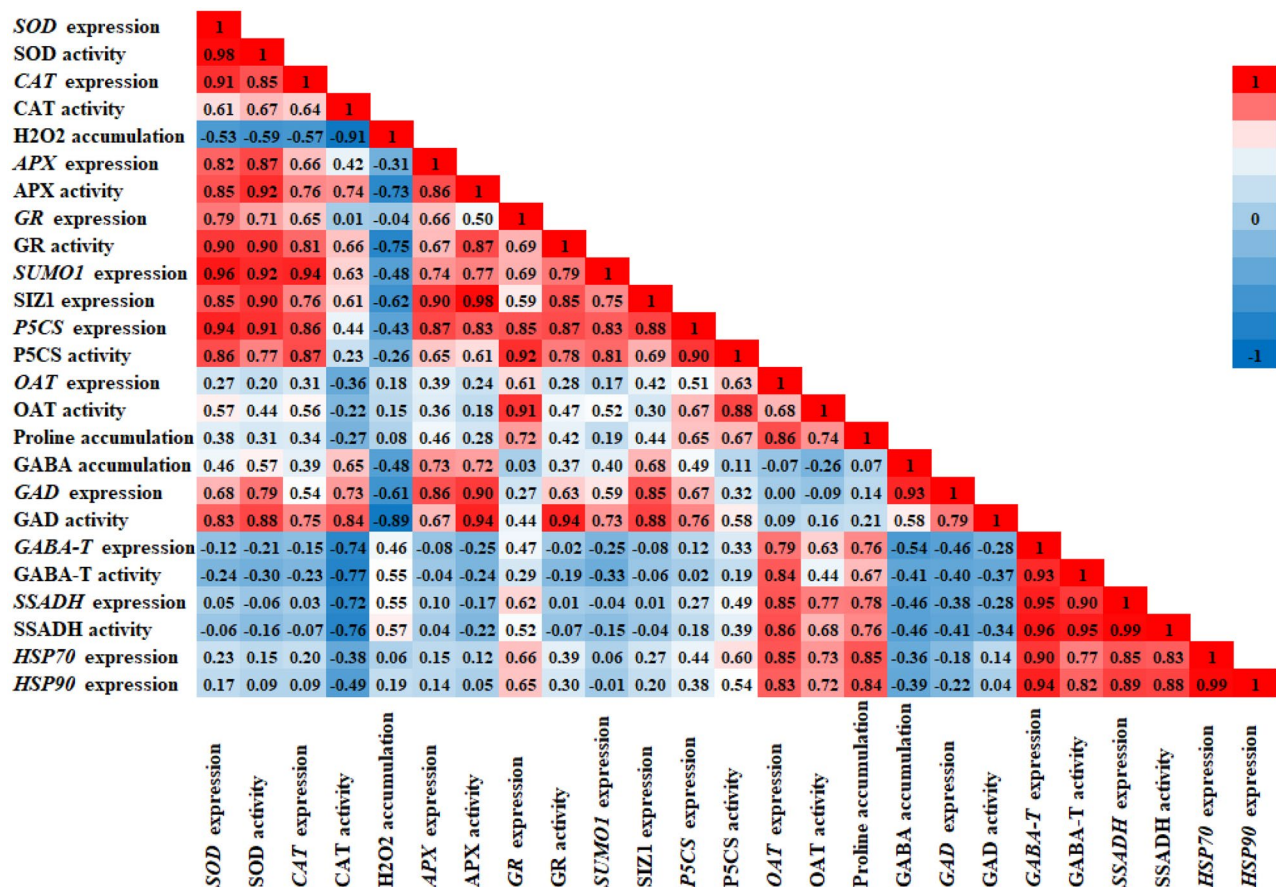


Figure 5. The Pearson correlation coefficient was calculated based on *SUMO1* and *SUMO E3 ligase SIZ1* genes expression, *SOD*, *CAT*, *APX* and *GR* genes expression and enzymes activity, *P5CS* and *OAT* genes expression and enzymes activity, *GAD*, *GABA-T* and *SSADH* genes expression and enzymes activity, and *HSP70* and *HSP90* genes expression accompanying by endogenous H_2O_2 , proline and GABA accumulation of cut rose flowers in response to 0 and 150 nM PSK α treatment.

for delaying senescence and prolonging the vase life of cut rose flower by exogenous PSK α application. However, deeply research is needed for understanding and elucidating post-translational regulatory mechanisms orchestrating petals senescence in rose flowers.

Conclusion

In our study, during flower bud opening, higher *SUMO1* and *SUMO E3 ligase SIZ1* genes expression were accompanied by (1) higher expression and activities of ROS scavenging *SOD*, *CAT*, *APX*, and *GR*, (2) higher proline accumulation due to higher *P5CS* gene expression and enzyme activity, and (3) higher GABA accumulation due to higher *GAD* expression and activity. After flowers are harvested, lower activity of *SUMO1*/*SUMO E3 ligase SIZ1* signaling pathway was associated with lower activity of ROS scavenging system and lower glutamate supply for proline and GABA accumulation, thereby accelerating petal senescence in rose flowers. Following the administration of PSK α treatment, postponing petal senescence in cut rose flowers could be ascribed to triggering *SUMO1* and *SUMO E3 ligase SIZ1* genes expression accompanied by higher activity of ROS scavenging system, higher accumulation of proline and GABA, and higher expression of *HSPs* (Fig. 5). Our results highlight the potential of the PSK α to be employed as a promising antisenesescence signaling peptide in the floriculture industry to extend the vase life of cut rose flowers.

Received: 18 August 2021; Accepted: 18 November 2021

Published online: 01 December 2021

References

- Aghdam, M. S., Ebrahimi, A., Sheikh-Assadi, M. & Naderi, R. Endogenous phyto-sulfokine α (PSK α) signaling delays petals senescence and prolongs vase life of cut rose flowers (*Rosa hybrida* cv. Angelina). *Sci. Hortic.* **289**, 110444. <https://doi.org/10.1016/j.scienta.2021.110444> (2021).
- Miura, K., Jin, J. B. & Hasegawa, P. M. Sumoylation, a post-translational regulatory process in plants. *Curr. Opin. Plant Biol.* **10**, 495–502. <https://doi.org/10.1016/j.pbi.2007.07.002> (2007).

3. Benlloch, R. & Lois, L. M. Sumoylation in plants: Mechanistic insights and its role in drought stress. *J. Exp. Bot.* **69**, 4539–4554. <https://doi.org/10.1093/jxb/ery233> (2018).
4. Miura, K. *et al.* SIZ1-mediated sumoylation of ICE1 controls CBF3/DREB1A expression and freezing tolerance in *Arabidopsis*. *Plant Cell* **19**, 1403–1414. <https://doi.org/10.1105/tpc.106.048397> (2007).
5. Wang, H. *et al.* OsSIZ1, a SUMO E3 ligase gene, is involved in the regulation of the responses to phosphate and nitrogen in rice. *Plant Cell Physiol.* **56**, 2381–2395. <https://doi.org/10.1093/pcp/pcv162> (2015).
6. Rytz, T. C. *et al.* SUMOylation profiling reveals a diverse array of nuclear targets modified by the SUMO ligase SIZ1 during heat stress. *Plant Cell* **30**, 1077–1099. <https://doi.org/10.1105/tpc.17.00993> (2018).
7. Zhang, S. *et al.* SUMO E3 ligase SIZ1 facilitates heat tolerance in tomato. *Plant Cell Physiol.* **59**, 58–71 (2018).
8. Castro, P. H. *et al.* SIZ1-dependent post-translational modification by SUMO modulates sugar signaling and metabolism in *Arabidopsis thaliana*. *Plant Cell Physiol.* **56**, 2297–2311. <https://doi.org/10.1093/pcp/pcv149> (2015).
9. Kim, J. Y. *et al.* Nitrate reductases are relocalized to the nucleus by AtSIZ1 and their levels are negatively regulated by COP1 and ammonium. *Int. J. Mol. Sci.* <https://doi.org/10.3390/ijms19041202> (2018).
10. Park, B. S., Song, J. T. & Seo, H. S. *Arabidopsis* nitrate reductase activity is stimulated by the E3 SUMO ligase AtSIZ1. *Nat. Commun.* **2**, 400. <https://doi.org/10.1038/ncomms1408> (2011).
11. Park, B. S., Kim, S. I., Song, J. T. & Seo, H. S. *Arabidopsis* SIZ1 positively regulates alternative respiratory bypass pathways. *BMB Rep.* **45**, 342–347. <https://doi.org/10.5483/bmbrep.2012.45.6.010> (2012).
12. Gong, Q. *et al.* SUMOylation of MYB30 enhances salt tolerance by elevating alternative respiration via transcriptionally upregulating AOX1a in *Arabidopsis*. *Plant J.* **102**, 1157–1171. <https://doi.org/10.1111/tpj.14689> (2020).
13. Zheng, T. *et al.* SUMO E3 Ligase SIZ1 stabilizes MYB75 to regulate anthocyanin accumulation under high light conditions in *Arabidopsis*. *Plant Sci.* **292**, 110355. <https://doi.org/10.1016/j.plantsci.2019.110355> (2020).
14. Zhou, L. J. *et al.* The small ubiquitin-like modifier E3 ligase MdSIZ1 promotes anthocyanin accumulation by sumoylating MdMYB1 under low-temperature conditions in apple. *Plant Cell Environ.* **40**, 2068–2080. <https://doi.org/10.1111/pce.12978> (2017).
15. Aghdam, M. S., Sayyari, M. & Luo, Z. Exogenous phyto-sulfokine α application delays senescence and promotes antioxidant nutrient accumulation in strawberry fruit during cold storage by triggering endogenous phyto-sulfokine α signaling. *Postharvest Biol. Technol.* **175**, 111473. <https://doi.org/10.1016/j.postharvbio.2021.111473> (2021).
16. Aghdam, M. S., Sayyari, M. & Luo, Z. Exogenous application of phyto-sulfokine α (PSKa) delays yellowing and preserves nutritional quality of broccoli florets during cold storage. *Food Chem.* **333**, 127481. <https://doi.org/10.1016/j.foodchem.2020.127481> (2020).
17. Aghdam, M. S., Flores, F. B. & Sedaghati, B. Exogenous phyto-sulfokine α (PSKa) application delays senescence and relieves decay in strawberry fruit during cold storage by triggering extracellular ATP signaling and improving ROS scavenging system activity. *Sci. Hortic.* **279**, 109906. <https://doi.org/10.1016/j.scienta.2021.109906> (2021).
18. Aghdam, M. S. & Luo, Z. Exogenous application of phyto-sulfokine α (PSKa) delays senescence in broccoli florets during cold storage by ensuring intracellular ATP availability and avoiding intracellular ROS accumulation. *Sci. Hortic.* **276**, 109745. <https://doi.org/10.1016/j.scienta.2020.109745> (2021).
19. Aghdam, M. S. & Flores, F. B. Employing phyto-sulfokine α (PSKa) for delaying broccoli florets yellowing during cold storage. *Food Chem.* **355**, 129626. <https://doi.org/10.1016/j.foodchem.2021.129626> (2021).
20. Wang, D. *et al.* Exogenous phyto-sulfokine α (PSKa) alleviates chilling injury of banana by modulating metabolisms of nitric oxide, polyamine, proline, and γ -aminobutyric acid. *Food Chem.* <https://doi.org/10.1016/j.foodchem.2020.127685> (2021).
21. Aghdam, M. S. & Alikhani-Koupaei, M. Exogenous phyto-sulfokine α (PSKa) applying delays senescence and relief decay in strawberry fruits during cold storage by sufficient intracellular ATP and NADPH availability. *Food Chem.* **336**, 127685. <https://doi.org/10.1016/j.foodchem.2020.127685> (2021).
22. Aghdam, M. S., Alikhani-Koupaei, M. & Khademian, R. Delaying broccoli floret yellowing by phyto-sulfokine α application during cold storage. *Front. Nutr.* **8**, 609217. <https://doi.org/10.3389/fnut.2021.609217> (2021).
23. Aghdam, M. S. & Luo, Z. Harnessing cGMP signaling pathways for improving fruits and vegetables marketability. *Sci. Hortic.* **291**, 110587. <https://doi.org/10.1016/j.scienta.2021.110587> (2022).
24. Giannopolitis, C. N. & Ries, S. K. Superoxide dismutases: I. Occurrence in higher plants. *Plant Physiol.* **59**, 309–314 (1977).
25. Beers, R. F. & Sizer, I. W. A spectrophotometric method for measuring the breakdown of hydrogen peroxide by catalase. *J. Biol. Chem.* **195**, 133–140 (1952).
26. Nakano, Y. & Asada, K. Hydrogen peroxide is scavenged by ascorbate-specific peroxidase in spinach chloroplasts. *Plant Cell Physiol.* **22**, 867–880 (1981).
27. Sofo, A., Tuzio, A. C., Dichio, B. & Xiloyannis, C. Influence of water deficit and rewetting on the components of the ascorbate–glutathione cycle in four interspecific *Prunus* hybrids. *Plant Sci.* **169**, 403–412. <https://doi.org/10.1016/j.plantsci.2005.04.004> (2005).
28. Patterson, B. D., MacRae, E. A. & Ferguson, I. B. Estimation of hydrogen peroxide in plant extracts using titanium(IV). *Anal. Biochem.* **139**, 487–492. [https://doi.org/10.1016/0003-2697\(84\)90039-3](https://doi.org/10.1016/0003-2697(84)90039-3) (1984).
29. Shan, T. *et al.* Exogenous glycine betaine treatment enhances chilling tolerance of peach fruit during cold storage. *Postharvest Biol. Technol.* **114**, 104–110. <https://doi.org/10.1016/j.postharvbio.2015.12.005> (2016).
30. Deewatthanawong, R., Rowell, P. & Watkins, C. B. γ -Aminobutyric acid (GABA) metabolism in CO₂ treated tomatoes. *Postharvest Biol. Technol.* **57**, 97–105. <https://doi.org/10.1016/j.postharvbio.2010.03.007> (2010).
31. Bartyzel, I., Pelczar, K. & Paszkowski, A. Functioning of the γ -aminobutyrate pathway in wheat seedlings affected by osmotic stress. *Biol. Plant.* **47**, 221–225 (2003).
32. Ansari, M. I., Lee, R. H. & Chen, S. C. G. A novel senescence-associated gene encoding γ -aminobutyric acid (GABA): Pyruvate transaminase is upregulated during rice leaf senescence. *Physiol. Plant.* **123**, 1–8 (2005).
33. Thorburn, D., Thompson, G. & Howells, D. A fluorimetric assay for succinic semialdehyde dehydrogenase activity suitable for prenatal diagnosis of the enzyme deficiency. *J. Inher. Metab. Dis.* **16**, 942–949 (1993).
34. Livak, K. J. & Schmittgen, T. D. Analysis of relative gene expression data using real-time quantitative PCR and the 2^{- Δ ACT} method. *Methods* **25**, 402–408 (2001).
35. IBM Corp. Released (2012). IBM SPSS Statistics for Windows, Version 21.0. Armonk, NY: IBM Corp.
36. Kolde, R. & Kolde, M. R. Package ‘pheatmap’. *R Package* **1**, 790 (2015).
37. Xiong, Y. *et al.* Glucose–TOR signalling reprograms the transcriptome and activates meristems. *Nature* **496**, 181–186. <https://doi.org/10.1038/nature12030> (2013).
38. Dong, Y. *et al.* Sulfur availability regulates plant growth via glucose–TOR signaling. *Nat. Commun.* **8**, 1174. <https://doi.org/10.1038/s41467-017-01224-w> (2017).
39. Schepetilnikov, M. *et al.* GTPase ROP2 binds and promotes activation of target of rapamycin, TOR, in response to auxin. *EMBO J.* **36**, 886–903 (2017).
40. Liu, Y. *et al.* Diverse nitrogen signals activate convergent ROP2–TOR signaling in *Arabidopsis*. *Dev. Cell* **56**, 1283–1295.e1285. <https://doi.org/10.1016/j.devcel.2021.03.022> (2021).
41. Tulin, F., Zhang, Z. & Wang, Z.-Y. Activation of TOR signaling by diverse nitrogen signals in plants. *Dev. Cell* **56**, 1213–1214. <https://doi.org/10.1016/j.devcel.2021.04.014> (2021).
42. Burkart, G. M. & Brandizzi, F. A tour of TOR complex signaling in plants. *Trends Biochem. Sci.* **46**, 417–428. <https://doi.org/10.1016/j.tibs.2020.11.004> (2021).

43. Chen, C. *et al.* An Ethylene-inhibited NF-YC transcription factor RhNF-YC9 regulates petal expansion in rose. *Hortic. Plant J.* **6**, 419–427. <https://doi.org/10.1016/j.hpj.2020.11.007> (2020).
44. Horibe, T. Approach towards the control of rose flower opening by light environment. *Hortic. Int. J.* <https://doi.org/10.15406/hij.2018.02.00052> (2018).
45. Crozet, P. *et al.* SUMOylation represses SnRK1 signaling in *Arabidopsis*. *Plant J* **85**, 120–133. <https://doi.org/10.1111/tpj.13096> (2016).
46. Wang, L., Sun, X., Luo, W. & Qian, C. Roles of C-repeat binding factors-dependent signaling pathway in jasmonates-mediated improvement of chilling tolerance of postharvest horticultural commodities. *J. Food Qual.* <https://doi.org/10.1155/2018/8517018> (2018).
47. Seifi, H. S. *et al.* Concurrent overactivation of the cytosolic glutamine synthetase and the GABA shunt in the ABA-deficient sitiens mutant of tomato leads to resistance against *Botrytis cinerea*. *New Phytol.* **199**, 490–504. <https://doi.org/10.1111/nph.12283> (2013).
48. Liang, X., Zhang, L., Natarajan, S. K. & Becker, D. F. Proline mechanisms of stress survival. *Antioxid. Redox Signal.* **19**, 998–1011 (2013).
49. Qiu, X. M., Sun, Y. Y., Ye, X. Y. & Li, Z. G. Signaling role of glutamate in plants. *Front. Plant Sci.* **10**, 1743. <https://doi.org/10.3389/fpls.2019.01743> (2019).
50. Meena, M. *et al.* Regulation of L-proline biosynthesis, signal transduction, transport, accumulation and its vital role in plants during variable environmental conditions. *Heliyon* **5**, e02952. <https://doi.org/10.1016/j.heliyon.2019.e02952> (2019).
51. Shelp, B. J., Aghdam, M. S. & Flaherty, E. J. γ -Aminobutyrate (GABA) regulated plant defense: Mechanisms and opportunities. *Plants* **10**, 1939 (2021).
52. Aghdam, M. S., Jannatizadeh, A., Luo, Z. & Paliyath, G. Ensuring sufficient intracellular ATP supplying and friendly extracellular ATP signaling attenuates stresses, delays senescence and maintains quality in horticultural crops during postharvest life. *Trends Food Sci. Technol.* **76**, 67–81. <https://doi.org/10.1016/j.tifs.2018.04.003> (2018).
53. Mishra, N. *et al.* Overexpression of the rice SUMO E3 ligase gene OsSIZ1 in cotton enhances drought and heat tolerance, and substantially improves fiber yields in the field under reduced irrigation and rainfed conditions. *Plant Cell Physiol.* **58**, 735–746 (2017).
54. Zhang, S. *et al.* A novel tomato SUMO E3 ligase, SIZ1, confers drought tolerance in transgenic tobacco. *J. Integr. Plant Biol.* **59**, 102–117. <https://doi.org/10.1111/jipb.12514> (2017).
55. Aghdam, M. S., Sevillano, L., Flores, F. B. & Bodbodak, S. The contribution of biotechnology to improving post-harvest chilling tolerance in fruits and vegetables using heat-shock proteins. *J. Agric. Sci.* **153**, 7–24. <https://doi.org/10.1017/s0021859613000804> (2013).
56. Aghdam, M. S., Sevillano, L., Flores, F. B. & Bodbodak, S. Heat shock proteins as biochemical markers for postharvest chilling stress in fruits and vegetables. *Sci. Hortic.* **160**, 54–64. <https://doi.org/10.1016/j.scienta.2013.05.020> (2013).
57. Miura, K. *et al.* Accumulation of antioxidants and antioxidant activity in tomato, *Solanum lycopersicum*, are enhanced by the transcription factor SLICE1. *Plant Biotechnol.* **29**, 261–269. <https://doi.org/10.5511/plantbiotechnology.12.0303b> (2012).
58. Yin, X. *et al.* BrrICE1. 1 is associated with putrescine synthesis through regulation of the arginine decarboxylase gene in freezing tolerance of turnip (*Brassica rapa* var. *rapa*). *BMC Plant Biol.* **20**, 1–16 (2020).
59. Kumar, N., Pal, M. & Srivastava, G. C. Proline metabolism in senescing rose petals (*Rosa hybrida* L. ‘First Red’). *J. Hortic. Sci. Biotechnol.* **84**, 536–540 (2009).
60. Aghdam, M. S., Naderi, R., Malekzadeh, P. & Jannatizadeh, A. Contribution of GABA shunt to chilling tolerance in anthurium cut flowers in response to postharvest salicylic acid treatment. *Sci. Hortic.* **205**, 90–96. <https://doi.org/10.1016/j.scienta.2016.04.020> (2016).
61. Ansari, M. I., Jalil, S. U., Ansari, S. A. & Hasanuzzaman, M. GABA shunt: A key-player in mitigation of ROS during stress. *Plant Growth Regul.* **94**, 131–149. <https://doi.org/10.1007/s10725-021-00710-y> (2021).
62. Bor, M. & Turkan, I. Is there a room for GABA in ROS and RNS signalling?. *Environ. Exp. Bot.* **161**, 67–73. <https://doi.org/10.1016/j.envexpbot.2019.02.015> (2019).
63. Zhen, S. *et al.* First Comprehensive proteome analyses of lysine acetylation and succinylation in seedling leaves of *Brachypodium distachyon* L. *Sci. Rep.* **6**, 31576–31576. <https://doi.org/10.1038/srep31576> (2016).
64. Jin, W. & Wu, F. Proteome-wide identification of lysine succinylation in the proteins of tomato (*Solanum lycopersicum*). *PLoS ONE* **11**, e0147586. <https://doi.org/10.1371/journal.pone.0147586> (2016).
65. Kwezi, L. *et al.* The phytosulfokine (PSK) receptor is capable of guanylate cyclase activity and enabling cyclic GMP-dependent signaling in plants. *J. Biol. Chem.* **286**, 22580–22588. <https://doi.org/10.1074/jbc.M110.168823> (2011).
66. Kaufmann, C. & Sauter, M. Sulfated plant peptide hormones. *J. Exp. Bot.* **70**, 4267–4277. <https://doi.org/10.1093/jxb/erz292> (2019).
67. Surabhi, G.-K. & Badajena, B. Recent advances in plant heat stress transcription factors. *Transcription Factors for Abiotic Stress Tolerance in Plants* (ed Wani, S. H.) 153–200 (Academic Press, 2020).
68. Timperio, A. M., Egidi, M. G. & Zolla, L. Proteomics applied on plant abiotic stresses: Role of heat shock proteins (HSP). *J. Proteomics* **71**, 391–411. <https://doi.org/10.1016/j.jprot.2008.07.005> (2008).
69. Gagné, J.-P. *et al.* Proteomic investigation of phosphorylation sites in poly (ADP-ribose) polymerase-1 and poly (ADP-ribose) glycohydrolase. *J. Proteome Res.* **8**, 1014–1029 (2009).
70. Martin, N. *et al.* PARP-1 transcriptional activity is regulated by sumoylation upon heat shock. *EMBO J.* **28**, 3534–3548 (2009).
71. Khaskheli, A. J. *et al.* RHERF113 functions in ethylene-induced petal senescence by modulating cytokinin content in rose. *Plant Cell Physiol.* **59**, 2442–2451. <https://doi.org/10.1093/pcp/pcy162> (2018).
72. Lu, P. *et al.* RhHB1 mediates the antagonism of gibberellins to ABA and ethylene during rose (*Rosa hybrida*) petal senescence. *Plant J.* **78**, 578–590. <https://doi.org/10.1111/tpj.12494> (2014).
73. Sun, X. *et al.* Molecular understanding of postharvest flower opening and senescence. *Mol. Hortic.* **1**, 7. <https://doi.org/10.1186/s43897-021-00015-8> (2021).
74. Heyman, J. *et al.* ERF115 controls root quiescent center cell division and stem cell replenishment. *Science* **342**, 860–863 (2013).
75. Kong, X. *et al.* PHB3 maintains root stem cell niche identity through ROS-responsive AP2/ERF transcription factors in *Arabidopsis*. *Cell Rep.* **22**, 1350–1363 (2018).
76. Galon, Y., Finkler, A. & Fromm, H. Calcium-regulated transcription in plants. *Mol. Plant* **3**, 653–669. <https://doi.org/10.1093/mp/ssq019> (2010).
77. Boulanger, M., Chakraborty, M., Tempé, D., Piechaczyk, M. & Bossis, G. SUMO and transcriptional regulation: The lessons of large-scale proteomic, modifomic and genomic studies. *Molecules (Basel, Switzerland)* **26**, 828. <https://doi.org/10.3390/molecules26040828> (2021).
78. Catala, R. *et al.* The *Arabidopsis* E3 SUMO ligase SIZ1 regulates plant growth and drought responses. *Plant Cell* **19**, 2952–2966. <https://doi.org/10.1105/tpc.106.049981> (2007).
79. Kim, D. Y., Han, Y. J., Kim, S. I., Song, J. T. & Seo, H. S. *Arabidopsis* CMT3 activity is positively regulated by AtSIZ1-mediated sumoylation. *Plant Sci.* **239**, 209–215. <https://doi.org/10.1016/j.plantsci.2015.08.003> (2015).
80. Miura, K. *et al.* Sumoylation of ABIS by the *Arabidopsis* SUMO E3 ligase SIZ1 negatively regulates abscisic acid signaling. *Proc. Natl. Acad. Sci.* **106**, 5418–5423 (2009).
81. Azad, A. K., Ishikawa, T., Ishikawa, T., Sawa, Y. & Shibata, H. Intracellular energy depletion triggers programmed cell death during petal senescence in tulip. *J. Exp. Bot.* **59**, 2085–2095. <https://doi.org/10.1093/jxb/ern066> (2008).

82. Rogers, H. J. Is there an important role for reactive oxygen species and redox regulation during floral senescence?. *Plant Cell Environ.* **35**, 217–233. <https://doi.org/10.1111/j.1365-3040.2011.02373.x> (2012).
83. Shibuya, K. Molecular aspects of flower senescence and strategies to improve flower longevity. *Breed. Sci.* **68**, 99–108. <https://doi.org/10.1270/jsbbs.17081> (2018).
84. Liu, J. *et al.* A RhABF2/Ferritin module affects rose (*Rosa hybrida*) petal dehydration tolerance and senescence by modulating iron levels. *Plant J* **92**, 1157–1169. <https://doi.org/10.1111/tbj.13751> (2017).

Author contributions

M.S.A.: Conceptualization, funding acquisition, project administration, M.S.A.: methodology, data curation, writing—original draft, Writing—review and editing. A.E.: Methodology, data curation, validation. M.S.-A.: Methodology, data curation, formal analysis, validation.

Competing interests

The authors declare no competing interests.


Additional information

Supplementary Information The online version contains supplementary material available at <https://doi.org/10.1038/s41598-021-02712-2>.

Correspondence and requests for materials should be addressed to M.S.A.

Reprints and permissions information is available at www.nature.com/reprints.

Publisher's note Springer Nature remains neutral with regard to jurisdictional claims in published maps and institutional affiliations.

 **Open Access** This article is licensed under a Creative Commons Attribution 4.0 International License, which permits use, sharing, adaptation, distribution and reproduction in any medium or format, as long as you give appropriate credit to the original author(s) and the source, provide a link to the Creative Commons licence, and indicate if changes were made. The images or other third party material in this article are included in the article's Creative Commons licence, unless indicated otherwise in a credit line to the material. If material is not included in the article's Creative Commons licence and your intended use is not permitted by statutory regulation or exceeds the permitted use, you will need to obtain permission directly from the copyright holder. To view a copy of this licence, visit <http://creativecommons.org/licenses/by/4.0/>.

© The Author(s) 2021